CFD MODELLING OF CONDENSATION OF VAPOUR IN THE PRESSURIZED PPOOLEX FACILITY

T.J.H. Pättikangas and J. Niemi

VTT Technical Research Centre of Finland, P.O.B. 1000, FI–02044 VTT, Finland

J. Laine, M. Puustinen and H. Purhonen

LUT Energy, Faculty of Technology, Lappeenranta University of Technology, Lappeenranta, Finland

Abstract

The behaviour of a pressure suppression containment is studied experimentally and by performing CFD calculations. The experiments have been performed with the PPOOLEX test facility, which is a scaled-down two-compartment model of a pressure suppression containment of a BWR. In the experiments, vapour is blown into the drywell compartment initially filled with air. When the pressure increases, the mixture of air and vapour flows through the vent pipe into the water pool of the wetwell compartment.

CFD simulation of the first 100 seconds of the experiment has been performed by using the Euler-Euler two-phase model of FLUENT code. In the model, the gas phase consists of air and vapour species components. In wall condensation, the condensing water forms a film layer on the wall surface, which is modelled by mass transfer from the gas phase to the liquid water phase in the near-wall grid cell. The heat transfer from the gas phase through the water film to the wall is resolved. The direct-contact condensation in the wetwell is modelled with a heat transfer coefficient. The calculated temperature, pressure and wall-condensation are compared to the results of the PPOOLEX experiment.

1. INTRODUCTION

In boiling water reactors (BWR), the major function of the containment system is to protect the environment if a loss-of-coolant accident (LOCA) should occur. The containment is designed to accommodate the loads generated in hypothetical accidents, such as sudden rupture of a main steam line. In such an accident, a large amount of steam is suddenly released in the containment. An essential part of the pressure suppression containment is a water pool, where condensation of released steam occurs.

In a BWR, the pressure suppression containment typically consists of a drywell and a wetwell with a water pool. In a hypothetical LOCA, steam and air flow from the drywell through vent pipes to the wetwell, where the outlets of the vent pipes are submerged in the water pool. In the early part of the accident, mainly non-condensable air or nitrogen flows through the vent pipes into the wetwell. Then, the volume fraction of vapour increases in the gas mixture. When all the non-condensable gas from the drywell has been blown into the wetwell, the blowdown consists of pure vapour. The pressure suppression pool changes this large volume of vapour to a small volume of liquid water (Lahey and Moody, 1993).

The PPOOLEX test facility is a scaled-down model of a pressure suppression containment of a BWR (Puustinen et al., 2009). The pressurized PPOOLEX vessel shown in Figure 1 consists of a drywell compartment and a wetwell compartment with a water pool. The compartments are connected with a vent pipe, whose outlet is submerged in the water pool in the wetwell. In experiments, vapour is generated with steam generators and blown into the drywell.

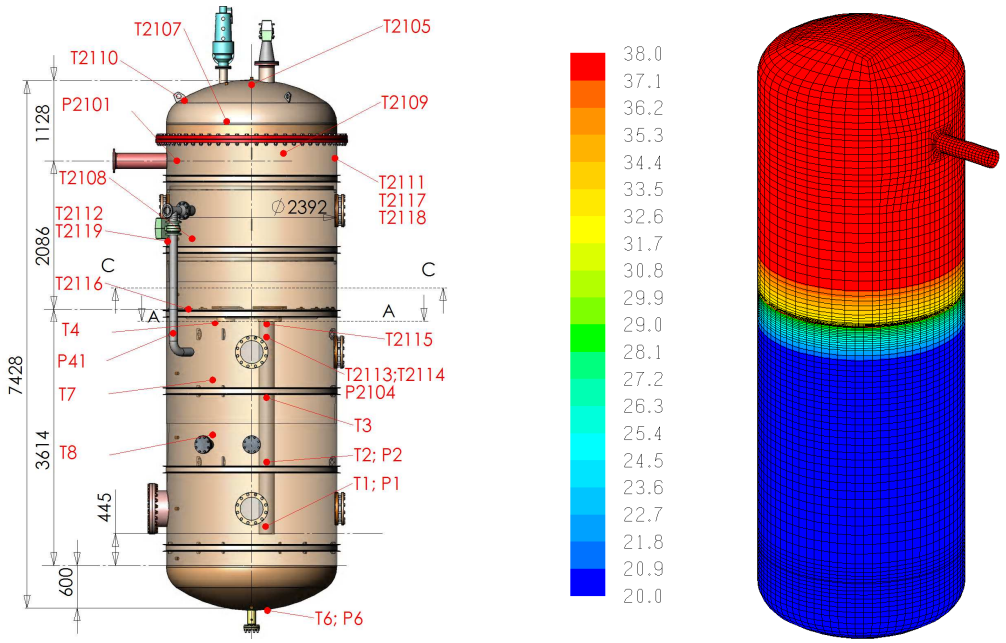

Fig. 1: Pressure (Pn) and temperature (Tn) measurements in the PPOOLEX pressurized test facility at Lappeenranta University of Technology. On the right, the surface mesh of the CFD model and the outer wall temperature (°C) at time t = 0 are shown.

In the PPOOLEX experiment WLL-05-02, vapour was blown into the preheated drywell compartment of the facility. The vapour jet hit the opposite wall of the drywell, where wall condensation occurred. The temperature of the wall structures of the drywell rose and heat was conducted through uninsulated walls to the ambient laboratory. When the pressure in the drywell increased, the mixture of air and vapour started flowing through the vent pipe into the water pool of the wetwell. The vent pipe was cleared of water and large gas bubbles formed at the pipe outlet with a frequency of about 1.4 hertz. The volume fraction of vapour in the drywell increased and direct-contact condensation at the outlet of the vent pipe became significant.

In the present work, a computational fluid dynamics (CFD) simulation of the first 100 seconds of the experiment is performed by using the Euler-Euler two-phase model of FLUENT (Fluent, 2006). In the model, the gas phase consists of air and vapour species components. In wall condensation, the condensing water forms a film layer on the wall surface, which is modelled by mass transfer from the gas phase to the liquid water phase in the near-wall grid cell. The heat transfer from the gas phase through the water film to the wall is resolved. The direct-contact condensation in the wetwell is modelled with a heat transfer coefficient. The wall condensation and direct-contact condensation models are implemented with user-defined functions in FLUENT.

In Section 2, the PPOOLEX facility and the experiment WLL-05-02 are described. The two-phase CFD models for condensation are described in Section 3. In Section 4, the CFD results for the experiment WLL-05-02 are presented and compared to the measurements. Finally, Section 5 contains a summary and discussion.

2. THE PPOOLEX TEST FACILITY

PPOOLEX is a pressurized cylindrical vessel with a height of 7.45 meters and a diameter of 2.4 meters. The volume of the drywell compartment is 13.3 m^3 and the volume of the wetwell

compartment is 17.8 m^3. The DN200 (∅219.1 × 2.5 mm) vent pipe is positioned in a non-axisymmetric location 300 mm away from the centre of the facility. The water level in the beginning of the experiments was 2.14 m from the bottom of the pool. The submergence depth of the DN200 vent pipe was 1.05 m, which corresponds to a hydrostatic pressure of about 10.2 kPa at the vent pipe outlet. The PPOOLEX facility is shown in Figure 1.

In the experiments, the drywell compartment was initially filled with air at atmospheric pressure. Preheating of the wall segments was executed with vapour. After preheating, the test vessel was shortly ventilated to dry the wall surfaces and to clear the viewing windows. In the experiments, pure vapour was blown into the drywell compartment of the PPOOLEX facility through the horizontal DN200 pipe. Vapour was obtained from the PACTEL steam generators connected to the DN200 pipe with a DN50 pipe. The mass flow rate of vapour into the drywell was measured with a vortex meter located in the DN50 line. In addition, the temperature of vapour was measured in the inlet plenum. The measured mass flow rate and temperature were used as boundary conditions in the CFD simulations.

Three different condensation phenomena occur in the experiments. First, some bulk condensation of vapour may occur, when vapour flows from the DN50 pipe through the DN200 inlet plenum into the drywell. Second, part of the vapour is condensed on the walls of the drywell. The wall condensation is determined by the initial wall temperature in the drywell and by the heat transfer through the uninsulated walls of the drywell to the laboratory. Third, direct-contact condensation occurs in the water pool of the wetwell.

3. CFD MODELS FOR CONDENSATION

The Euler-Euler model of FLUENT 6.3 was used in modelling the experiment. In the Euler-Euler model, the conservation equations of mass, momentum and enthalpy are solved for the gas phase and liquid phase. The gas phase is wet air, which consists of two species components: dry air and vapour. Gas phase is treated as a compressible ideal gas, where wall condensation, direct-contact condensation and bulk condensation are modelled with user-defined functions of FLUENT. Different implementations of wall-condensation models were recently benchmarked by Ambrosini et al. (2008). The direct-contact condensation models have been reviewed by Kim et al. (2004).

3.1 Wall-condensation

The idea of the diffusive wall-condensation model is illustrated in Fig. 2, where the mass and energy balances at the gas-liquid interface are shown. In condensation or evaporation, the mass balance reads

$$\dot{m}''_{\text{steam}} = \dot{m}''_{\text{water}} \qquad (1)1$$

where $\dot{m}''_{\text{steam}}$ is the mass sink or source in the gas phase and $\dot{m}''_{\text{water}}$ is the mass source or sink in the liquid phase. The energy balance at the interface is

$$Q''_{\text{gas}} + \dot{m}''_{\text{steam}} h_{\text{steam}}(T_{\text{steam}}) = Q''_{\text{liquid}} + \dot{m}''_{\text{water}} h_{\text{water}}(T_{\text{water}}) \qquad (2)$$

where T_{steam} and T_{water} depend on the direction of the mass transfer (i.e., condensation/evaporation).

In condensation, steam disappears at the gas temperature T_{gas} and water appears at the interface temperature T_{i} . In evaporation, steam appears at the interface temperature T_{i} and water disappears at the liquid temperature T_{liquid}.

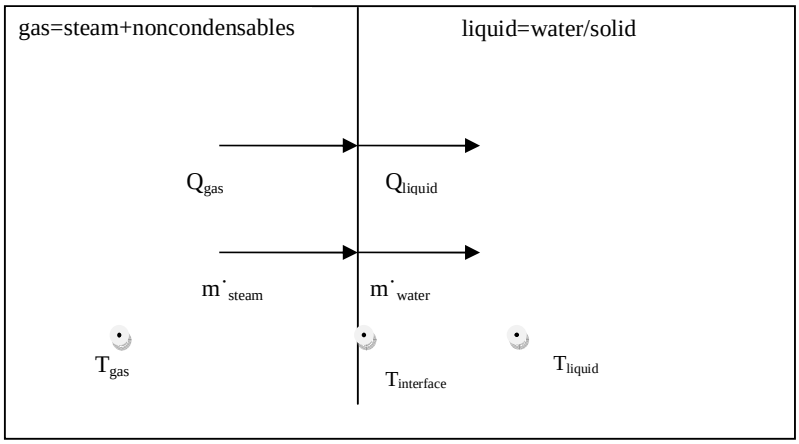

Fig. 2: Heat transfer from the gas phase through the liquid film to the solid wall.

The heat flux densities are determined by

$$\begin{aligned} Q''_{\text{gas}} &= htc_{\text{gas}}(T_{\text{gas}} - T_{\text{i}}) \\ Q''_{\text{liquid}} &= htc_{\text{liquid}}(T_{\text{i}} - T_{\text{liquid}}) \end{aligned} \tag{3}$$

The condensation mass flux density is determined by near-wall diffusion

$$\dot{m}''_{\text{steam}} = -\frac{w_{\text{steam}}}{w_{\text{mixture}}} mtc \cdot \ln\left(\frac{1-y_{\text{steam}}}{1-y_{\text{i}}}\right) \tag{4}$$

where y_{steam} is the mole fraction of steam in the near-wall grid cell and y_{i} is the mole fraction of steam in the interface. The turbulent mass transfer coefficient is *mtc* and w_{steam} and w_{mixture} are the molecular weights of steam and mixture, respectively. The mole fraction of steam at the interface is a function of the interface temperature:

$$y_{\text{i}}(T_{\text{i}}) = p_{\text{sat}}(T_{\text{i}}) / p_{\text{tot}} \tag{5}$$

The interface temperature T_{i} is determined by using Eqs (3)–(6) so that Eq. (2) is satisfied.

3.2 Direct-contact condensation

A simple model was used for describing the direct-contact condensation in the water pool. The model is intended to describe the basic features of direct-contact condensation in two-phase simulations with FLUENT.

The properties of the phases (T_{gas}, y_{steam}, T_{liquid}) and the heat transfer coefficients (htc_{gas} , htc_{liquid}) are assumed to be known. The gas phase is treated as a two component mixture, comprising of a condensable and a non-condensable gas component. The effects of the components to the heat transfer are estimated from the volume fractions of the components, i.e., the heat transfer area is reduced by the mole fraction (y_{air}, y_{steam}) of the component. The mass and heat transfer at the gas-liquid interface is determined by the phase properties (T_{gas}, T_{liquid}) of the fluid.

The mass balance at the interface is again given by Eq. (1). The energy balance at the interface is

$$Q''_{\text{air}} + Q''_{\text{steam}} + \dot{m}''_{\text{steam}} h_{\text{steam}}(T_{\text{steam}}) = Q''_{\text{noncond}} + Q''_{\text{water}} + \dot{m}''_{\text{water}} h_{\text{water}}(T_{\text{water}}) \tag{6}$$

where T_{steam} and T_{water} depend on the direction of mass transfer. In condensation, steam disappears at the gas temperature T_{gas} and water appears at the saturation temperature T_{sat} . In evaporation, steam appears at the saturation temperature T_{sat} and water disappears at the liquid temperature T_{liquid}. The enthalpies are estimated by Eq. (3), where the interface temperature is $T_i = T_{sat}$.

The heat transfer of the non-condensable gas component is determined by

$$Q''_{air} = Q''_{noncond} = y_{air} \frac{htc_{gas} \cdot htc_{liquid}}{htc_{gas} + htc_{liquid}} \left(T_{gas} - T_{liquid}\right) \tag{7}$$

The condensation or evaporation is determined by the saturation temperature of the condensable gas component:

$$T_{sat} = T_{sat}(p_{steam}) \tag{8}$$

The heat flux densities are

$$Q''_{steam} = y_{steam} \cdot htc_{gas} \left(T_{gas} - T_{sat}\right) \tag{9}$$

$$Q''_{water} = y_{steam} \cdot htc_{liquid} \left(T_{sat} - T_{liquid}\right) \tag{10}$$

When condensation occurs, i.e., $Q''_{water} > Q''_{steam}$, the mass flux density of steam is

$$\dot{m}''_{steam} = \frac{Q''_{water} - Q''_{steam}}{h_{steam}(T_{steam}) - h_{water}(T_{sat})} \tag{11}$$

When evaporation occurs, the mass flux density of steam is

$$\dot{m}''_{steam} = \frac{Q''_{water} - Q''_{steam}}{h_{steam}(T_{sat}) - h_{water}(T_{water})} \tag{12}$$

In the FLUENT model, a volumetric mass transfer rate is needed, which is obtained by multiplying the mass flux by area density. The area density is estimated by $ai = |\nabla \alpha|$, where α is the void fraction. In the present simulation, the heat transfer coefficient of gas has a constant value of htc_{gas} = 1000 W/m^2. The heat transfer coefficient for liquid is calculated from the correlation of Chen and Mayinger: $htc_{liquid} = 0.185\,\mathrm{Re}^{0.7}\,\mathrm{Pr}^{0.5}$.

4. CFD MODELLING OF THE EXPERIMENT WLL-05-02

The CFD mesh of the PPOOLEX facility consists of 135 000 hexahedral grid cells. The surface mesh is shown in Fig. 1. The QUICK scheme was used for the spatial discretization of the volume fraction equation and the second order upwind scheme for other variables. The first order implicit method was used for the time discretization with a time step 0.01 s. The gas phase was modelled as compressible ideal gas, and the floating operating pressure option of FLUENT was used.

The interfacial drag was modelled by using the symmetric drag model of FLUENT (Fluent, 2006). In the near-wall grid cells of the drywell, a large droplet size (d_p = 4 mm) was used so that liquid water was flowing downwards along the wall. The thickness of the liquid film on the wall was estimated from the amount of liquid water in the near-wall grid cell.

In the PPOOLEX experiment WLL-05-02, vapour was blown into the preheated drywell compartment of the facility. The initial temperature of the drywell was about 65 °C, and the initial temperature of the water pool in the wetwell was about 20 °C. The initial mole fraction of vapour in the gas phase was y_{steam} = 0.01. Temperature of the ambient laboratory was 25 °C. The convective heat transfer coefficient from the uninsulated wall to the ambient laboratory was assumed to be 4.53 W/m^{2}K, and the emissivity of the outer wall was assumed to be ε = 0.3. The thickness of the steel wall of the drywell was 8 mm.

In the experiment, the gas jet was injected into the drywell through the inlet plenum. In the CFD calculation, the gas was assumed to be almost pure vapour containing a mass fraction of one percent of air. The maximum mass flow rate of the jet was 0.54 kg/s, and the vapour temperature in the inlet plenum was about 140 °C. The mass flow rate into the drywell is shown in Fig. 3.

When the pressure in the drywell increases, the water plug in the vent pipe starts moving downwards. The vent pipe is cleared at time t = 3 s and the first bubble is formed at the outlet of the vent pipe in the water pool. After this, new bubbles are formed with a period of about 0.72 s. The periodic formation of bubbles can be clearly seen in the sinusoidal mass flow rate through the vent pipe that is shown in Fig. 3. When bubbles are detached from the vent outlet, the mass flow rate in the vent pipe becomes for awhile almost zero or is even reversed.

In Fig. 4, the shape of the gas bubble at the vent outlet is shown at a few instants of time. The calculated shapes of bubbles are quite similar to the ones observed in experiments. The calculated interface between the phases is, however, quite diffuse, when the bubbles are compared to those calculated earlier with the Volume Of Fluid (VOF) method (Pättikangas et al., 2009). The diffusive nature of the Euler-Euler method clearly affects the result.

In Fig. 5, the temperature of the gas phase is shown at a few instants of time. The initial temperature of the preheated drywell is somewhat stratified. Some heat conduction occurred through the floor of the drywell to the top part of the wetwell. The temperature was initialized to correspond to the measured temperatures at time t = 0. The initial temperature of the outer wall is shown in Fig. 1. The hot steam jet injected into the drywell bends slightly downwards before hitting the opposite wall of the drywell. The velocity of the steam jet is about 25 m/s. The temperature of the drywell rises during the first 100 s to about 120 °C.

In Fig. 6, the mole fraction of vapour in the gas phase is shown. The mole fraction of vapour increases rapidly from its initial value of one percent, and at time t = 100 s it is about 90% in the drywell. At this time, the gas flowing through the vent pipe into the water pool contains almost 80 % of vapour. Strong condensation of vapour occurs on the walls of the drywell and on the walls of the vent pipe that is submerged in cold water.

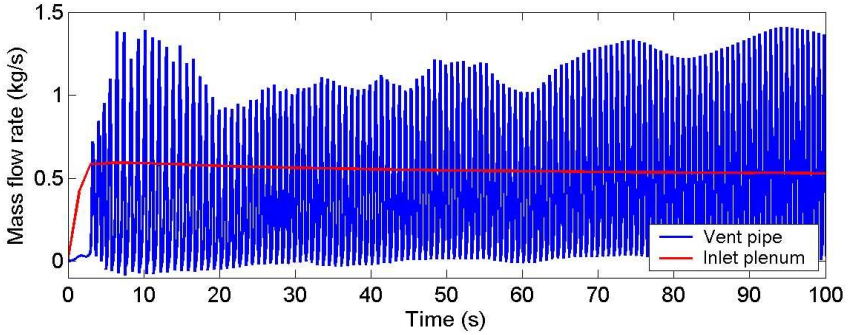

Fig. 3: Mass flow rate into the drywell (red line) and through the vent pipe (blue line).

t = 10 s

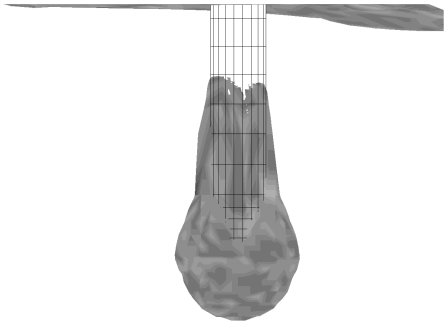

t = 10.0 s

20 s

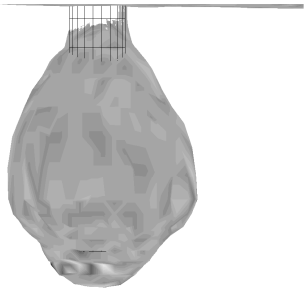

20.0 s

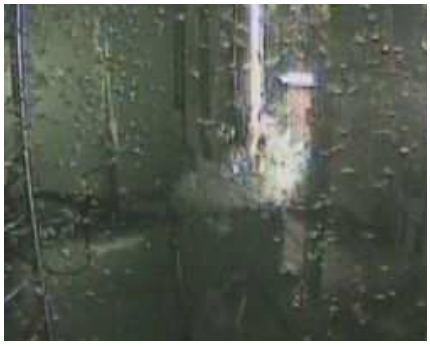

80 s

79.8 s

100 s

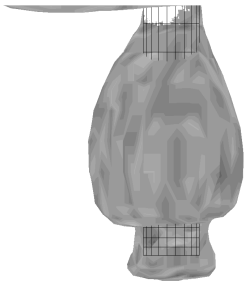

100.0 s

Fig. 4: Photographs of gas bubbles in the water pool during the experiment WLL-05-02. On the right, iso-surfaces of void fraction in the CFD simulation are shown ($\alpha = 0.1$).

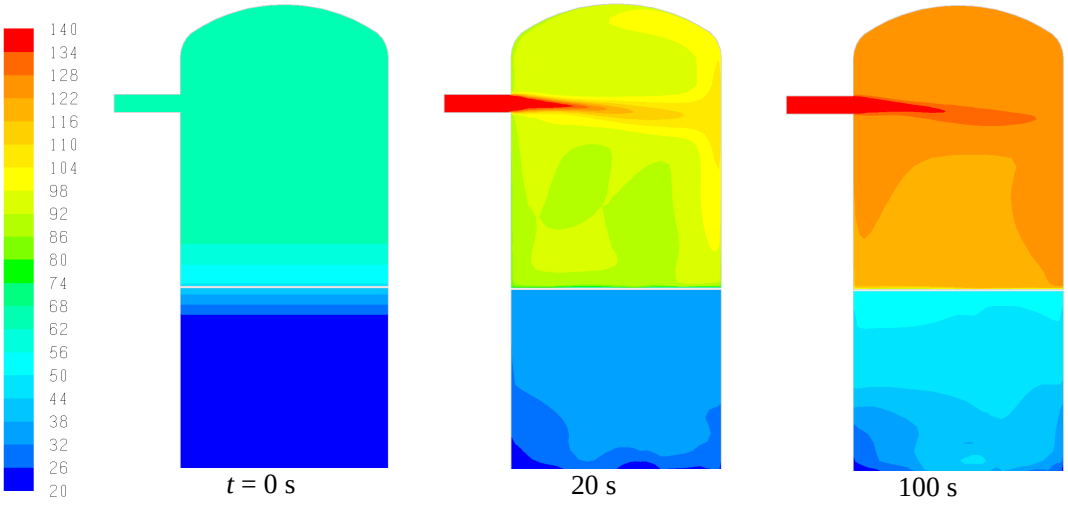

Fig. 5: Temperature of gas (°C) in the cross-section of the inlet plenum at a few instants of time.

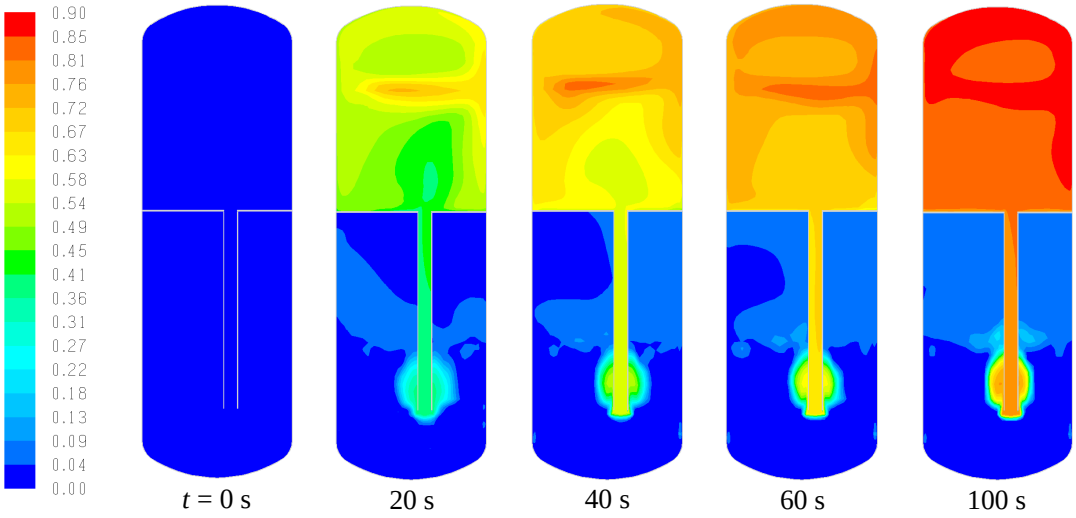

Fig. 6: Mole fraction of vapour in the cross-section of the vent pipe at different instants of time.

In Fig. 7, the wall condensation is shown on the back wall of the drywell, where the injected vapour jet hits. In the beginning of the experiment, the wall is fairly cold. Therefore, condensation is first strong and decreases gradually. The maximum condensation rate is about 3.6 kg/m^{2}s, and it occurs at time t = 18...22 s.

In Fig. 8, the direct-contact condensation rate at the outlet of the vent pipe is illustrated at a few instants of time. In the early phase of the experiment, the gas flowing through the vent pipe contains mainly air and, therefore, almost no condensation occurs. Later in the experiment, when the gas in the vent pipe contains mainly vapour, strong condensation occurs near the outlet of the vent pipe. The condensation is still affected by air, which has a mole fraction of about 20 %.

In the experiment, wall condensation in the drywell is studied by collecting condensate from the wall with a gutter system. The cumulative amount of condensate on the back wall, where the vapour jet hits first, is collected from a wall area of 5.25 m^2. The condensate from the front wall, where the inlet plenum is located, is also collected from a wall area of 5.25 m^2. The flow of condensate through the gutter system to the tanks causes a delay of about 25 s in the experiment.

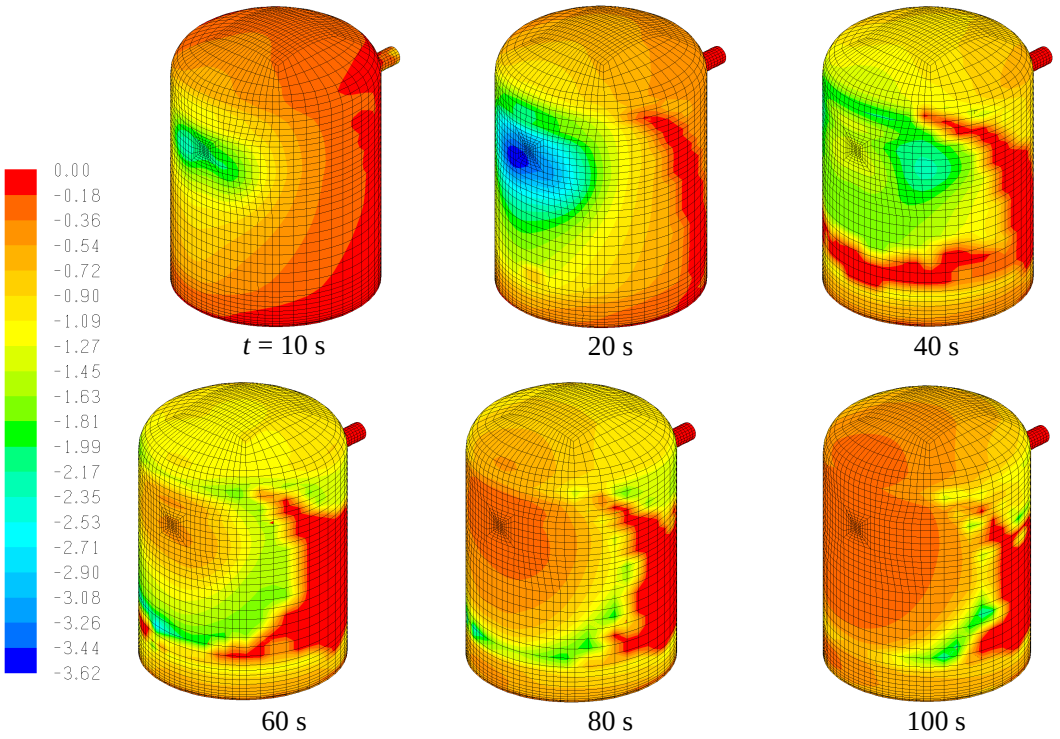

Fig. 7: Mass transfer rate (kg/m^{2}s) between the gas and liquid phases in wall condensation.

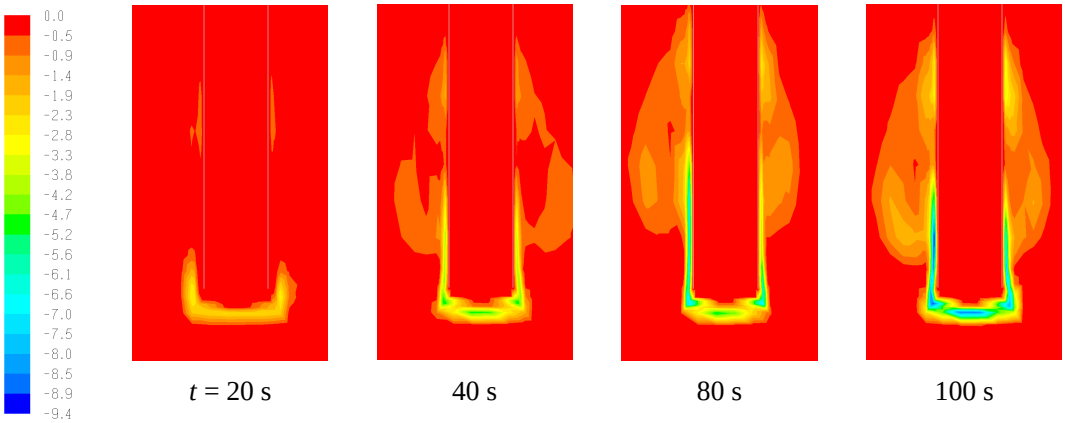

Fig. 8: Mass transfer rate (kg/m^{3}s) between the gas and liquid phases during direct-contact condensation at the outlet of the vent pipe.

The calculated results are compared to the measurements in Fig. 9, where the cumulative amount of condensate is shown. On the back wall, the condensation is slightly overestimated by the CFD calculation. On the front wall, the condensation is clearly underestimated by the calculation. In the total amount of condensation, the errors partly cancel each other. The calculated total amount of condensation is about 10% smaller than the measured value.

The PPOOLEX facility was uninsulated when the experiment was performed. In the early phase of the experiment, the amount of wall condensation is determined by heat transfer from the gas to the solid structures of the facility. Later, the heat transfer from the outer wall to the ambient laboratory determines the amount of condensation. The heat transfer to the laboratory is only modelled with a convective heat transfer coefficient and an emissivity for radiation heat transfer.

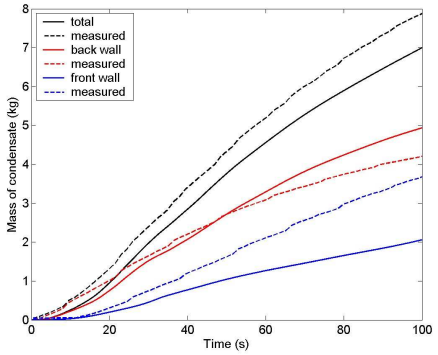

Fig. 9: The cumulative mass of condensate.

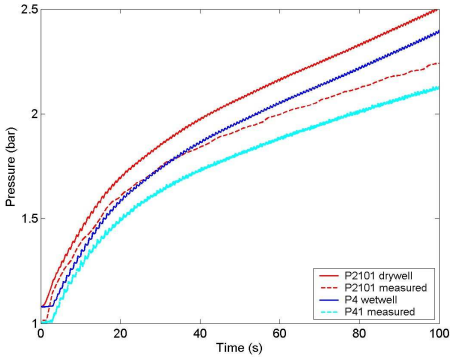

Fig. 10: Calculated and measured pressures in the drywell and wetwell.

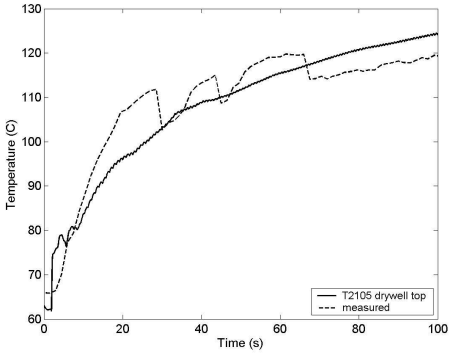

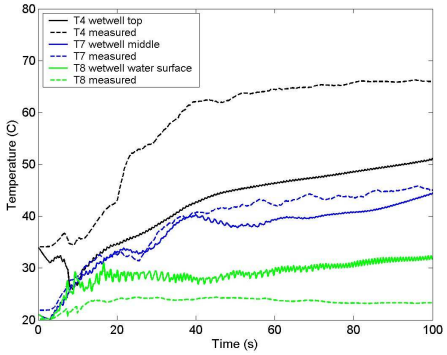

Fig. 11: Calculated and measured temperatures in the drywell (left) and wetwell (right).

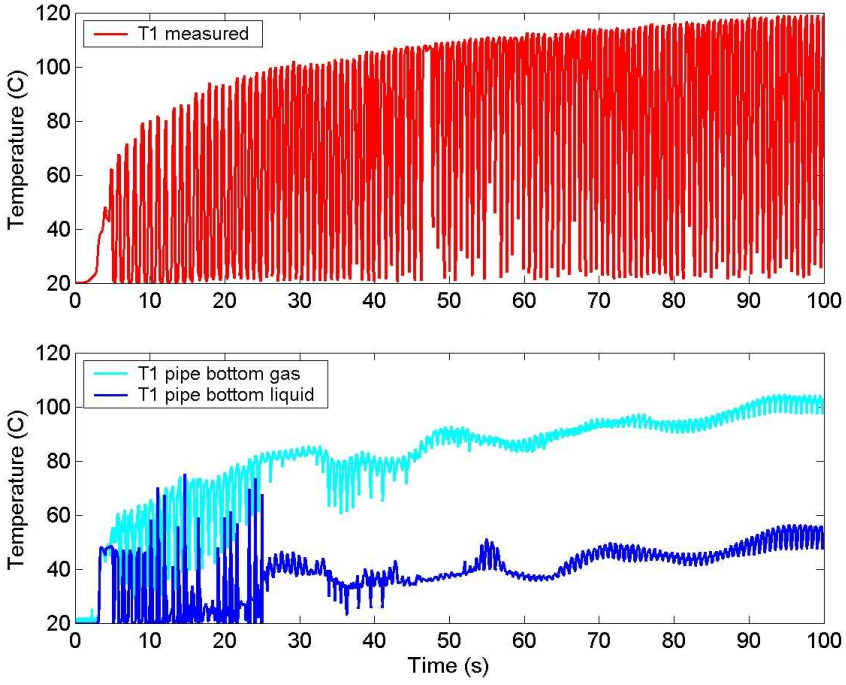

Fig. 12: Measured temperature in the vent pipe (top) and calculated temperatures of gas and liquid (bottom).

In Fig. 11, the calculated temperatures are compared to measurements at a few points in the drywell and wetwell. In the drywell, the measurement shows a few abrupt changes of temperature which are not captured by the calculation. Otherwise, the calculated temperature in the drywell is quite close to the measurement.

In the wetwell, the temperature of the gas space is stratified already in the beginning of the experiment. The measurements show that the stratified condition persists all the time during the experiment. In the calculation, more mixing occurs and stratification is weaker. The calculated temperature at the top of the wetwell drops already in the beginning of the calculation and differs from the measurement.

In Fig. 12, the measured temperature inside the vent pipe is shown. The measurement is done near the outlet of the pipe, where the sensor is initially submerged in water. When bubbles are forming at the outlet of the vent pipe, hot gas is surrounding the sensor. When the bubbles detach from the vent outlet, water flows into the vent pipe surrounding the sensor. Therefore, the sensor alternates in measuring the temperature of gas and water.

In the bottom part of Fig. 12, the calculated temperatures of gas and water are shown. The calculated temperatures of gas are somewhat lower than the measurements. The calculated temperature of water is higher than the measured value. This indicates that the calculated mixing of water near the vent outlet is not quite as strong as it is in reality.

The calculated pressures are compared to the measurements in Fig. 10. The calculated pressures are clearly higher than the measured values. The reason for this is the too small amount of wall condensation in the drywell, which in turn is caused by too weak heat transfer to the ambient laboratory. In addition, the direct-contact condensation in the water pool is also too weak. In Fig. 6, one can see that some vapour escapes through the water pool to the gas space of the wetwell. This is not observed to occur in reality. The reasons for this are the challenges in modelling the interfacial area and the interfacial heat transfer in the water pool.

5. SUMMARY AND DISCUSSION

CFD modelling has been performed for an experiment performed with the PPOOLEX test facility, which is a scaled-down model of a BWR pressure suppression containment. Models for wall condensation and direct-contact condensation have been implemented in the FLUENT code. The models have been tested against the PPOOLEX experiment WLL-05-02.

Comparison of the wall condensation model to the experiment was complicated by the uninsulated wall of the drywell of PPOOLEX. When the wall structures have been heated by the hot vapour, the wall condensation is determined by the heat transfer from the outer wall of the drywell to the ambient laboratory. In the CFD model, the chosen heat transfer coefficient on the outer wall determines the amount of condensation. In the calculation, this also affects the pressure level inside the drywell and wetwell.

In modelling the direct-contact condensation, the challenges are in the estimation of the interfacial surface area and the heat transfer coefficient. The heat transfer and condensation in the present calculation was found to be too weak. Some vapour was able to escape from the water pool to the gas space of the wetwell. An additional challenge is presented by modelling the interfacial drag in the different regions. In the drywell, some mist is formed by the bulk condensation. In the water pool, at the outlet of the vent pipe a large bubble is formed. In addition, small air bubbles are carried away by the flow in the water pool. More work is needed in order to find suitable modelling techniques for these phenomena.

An attempt was made to follow the Best Practise Guidelines in performing the calculations. A finer mesh size was used near the walls of the drywell and near the inner and outer surfaces of the

vent pipe in order to achieve small enough y^+ values. One of the problematic regions is the vent pipe, where the flow velocity and the y^+ value vary from very small values (< 1) to values of about 200. When a finer mesh is used near the outlet of the vent pipe, the bubble shape is reproduced somewhat more accurately than in the present calculations. Using a finer mesh in this region leads to a smaller time step and increased computing time. Therefore, the finer mesh was not used in these lengthy calculations.

The second order upwind scheme was used for the spatial discretization of all variables except for the void fraction, which was discretized by using the QUICK scheme. First order implicit scheme was used in the time discretization. The transient calculation would benefit from using the more accurate second order time discretization, but this was not used because of numerical stability.

The Euler-Euler model of FLUENT was used in the present simulations because it has separate enthalpy equations for each phase. This is necessary in modelling the heat and mass transfer between the phases. In modelling pressure suppression pools, the Volume Of Fluid (VOF) method is usually used (Hirt and Nichols, 1981; Yan and Bolger, 2010). The VOF method is suitable for modelling the beginning of the discharge, when non-condensable gas flows into the water pool. The large bubbles at the outlet of the vent pipe are described better by the VOF model than the more diffusive Euler-Euler model. On the other hand, in the experiments small bubbles of non-condensable gas are observed in the water pool, which cannot be captured by the VOF model.

Acknowledgements: This work has been done in the SAFIR2010 research programme (The Finnish Research Programme on Nuclear Power Plant Safety 2007–2010). The work has been funded by the Ministry of Employment and the Economy, VTT Technical Research Centre of Finland, Nordic Nuclear Safety Research (NKS) and Nordic Nuclear Reactor Thermal-Hydraulics Network (NORTHNET).

REFERENCES

W. Ambrosini, M. Bucci, N. Forgione, et al., "Comparison and analysis of the condensation benchmark results", *3rd European Review Meeting on Severe Accident Research (EMSAR-2008)*, Nesseber, Bulgaria, 23–25 September, 2008.

C.W. Hirt and B.D. Nichols, "Volume of fluid (VOF) method for the dynamics of free boundaries. *Journal of Computational Physics*, **39**, 201–225 (1981).

Fluent, *Fluent 6.3 User's Guide*, Fluent Inc., Lebanon, USA (2006).

Y.-S. Kim, J.-W. Park and C.-H. Song, "Investigation of the steam-water direct contact condensation heat transfer coefficients using interfacial transport models", *Int. Comm. Heat Mass Transfer*, **31**, 397–408 (2004).

R.T. Lahey and F.J. Moody, *The thermal hydraulics of a boiling water nuclear reactor*. 2nd Edition, American Nuclear Society (1993).

M. Puustinen, J. Laine, A. Räsänen and H. Purhonen, "PPOOLEX wall condensation experiments", *SAFIR2010, The Finnish Research Programme on Nuclear Power Plant Safety 2007–2010, Interim Report* (Ed. E.K. Puska), VTT Research Notes 2466, Technical Research Centre of Finland, Espoo, pp. 228–236 (2009).

T. Pättikangas, J. Niemi and A. Timperi, "Numerical modeling of condensation pool", ibid., pp. 160–172 (2009).

J. Yan and F. Bolger, "Evaluation of pool swell velocity during large break loss of coolant accident in boiling water reactor Mark III containment design", Nuclear Engineering and Design **240**, 1789–1794 (2010).